A.V.Kotikov, JINR, Dubna

(in collab. with B.G. Shaikhatdenov, JINR, Dubna and Pengming Zhang,
Institute of Modern Physics, Lanzhou)

based on Phys.Rev.D96 (2017) no. 11, 114002 (arXiv:1706.01849)

The XXIV International Baldin Seminar on High Energy Physics Problems
"Relativistic Nuclear Physics and Quantum Chromodynamics"

Dubna, September 17-22, 2018

EMC effect at small Bjorken x values

OUTLINE

1. Introduction
2. Results
3. Conclusions and Prospects

GENERAL

The Bessel-inspired behavior of parton densities at small Bjorken x values, obtained in the case of the flat initial conditions for DGLAP evolution equations, is used along with "frozen" and analytic modifications of the strong coupling constant to study the so-called EMC effect. Among other results, this approach allowed predicting small x behavior of the gluon density in nuclei.

1. Introduction to DIS

A. Deep-inelastic lepton-hadron scattering

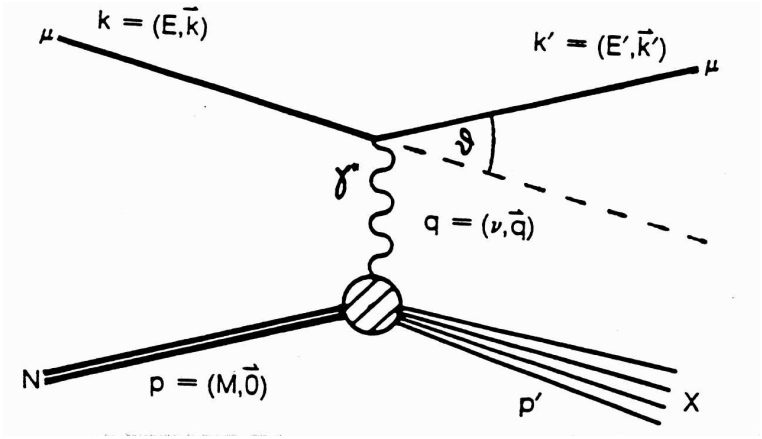

Deep-inelastic scattering cross-section:

$$\sigma \sim L^{\mu\nu} F^{\mu\nu}$$

Hadron part $F^{\mu\nu}$ ($Q^2 = -q^2 > 0$, $x = Q^2/[2(pq)]$):

$$F^{\mu\nu} = (-g^{\mu\nu} + \frac{q^\mu q^\nu}{q^2})F_1(x, Q^2)$$
$$- (p^\mu - \frac{(pq)}{q^2}q^\mu)(p^\nu - \frac{(pq)}{q^2}q^\nu)\frac{2x}{q^2}F_2(x, Q^2) + ...,$$

where $F_k(x, Q^2)$ ($k = 1, 2, 3, L$) - are DIS SF and q and p are photon and hadron (parton) momentums.

B. Wilson operator expansion: Mellin moments $M_k(n, Q^2)$ of DIS SF $F_k(x, Q^2)$ can be represented as sum

$$M_k(n, Q^2) = \sum_{a=NS,SI,g} \underbrace{C_k^a(n, Q^2/\mu^2)}_{\text{Coeff. function}} A_a(n, \mu^2),$$

where $A_a(n, \mu^2) =< N|\mathcal{O}^a_{\mu_1,\ldots,\mu_n}|N >$ are matrix elements of the Wilson operators $\mathcal{O}^a_{\mu_1,\ldots,\mu_n}$.

!!! **There is a factorization in the Mellin-moment space $\rightarrow$ there are Mellin convolutions in Bjorken-x space** !!!

C. The matrix elements $A_a(n,\mu^2)$ are Mellin moments of the unpolarized PDF $f_a(n,\mu^2)$.

DGLAP [= Renormgroup] equations:

$$\frac{d}{d\ln Q^2} f_a(x,Q^2) = \int_x^1 \frac{dy}{y} \sum_b W_{b\to a}(x/y)\, f_b(y,Q^2)\,. \qquad (1)$$

The anomalous dimensions (ADs) $\gamma_{ab}(n)$ of the twist-2 Wilson operators $\mathcal{O}^a_{\mu_1,\ldots,\mu_n}$ (hereafter $a_s = \alpha_s/(4\pi)$)

$$\gamma_{ab}(n) = \int_0^1 dx\; x^{n-1} W_{b\to a}(x) = \sum_{m=0}^{\infty} \gamma_{ab}^{(m)}(n) a_s^m,$$

All parton densities are multiplies by x, t.e.

structure function = combination of parton densities.

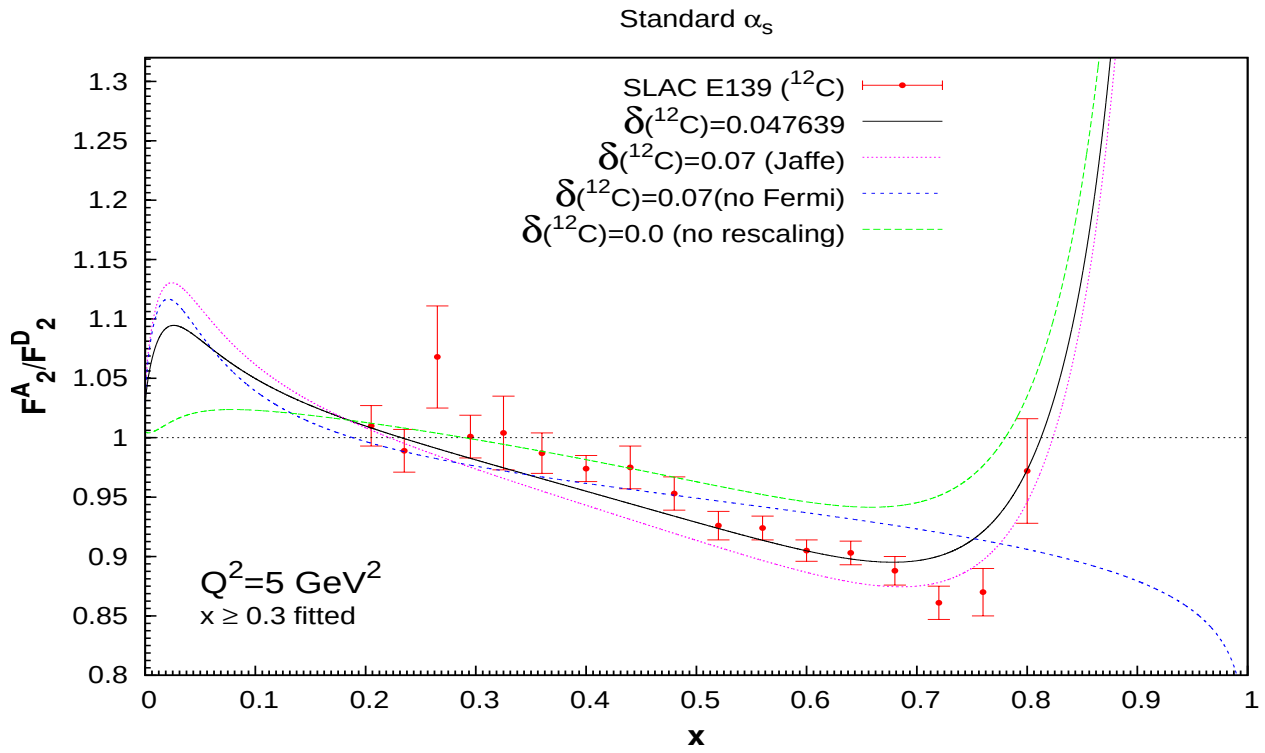

Figure 1: x dependence of the ratio $F_2^C(x,Q^2)/F_2^D(x,Q^2)$ in bins of x. The combined experimental data from SLAC E139 Collaboration are compared with the Fermi-Motion prediction (green line), rescaling model predictions (blue dashed line).

2 Introduction to EMC effect

The study of deep-inelastic scattering (DIS) of leptons off nuclei reveals an appearance of a significant nuclear effect.

(for a review see, e.g., (M. Arneodo,1992); (P.R. Norton, 2013);

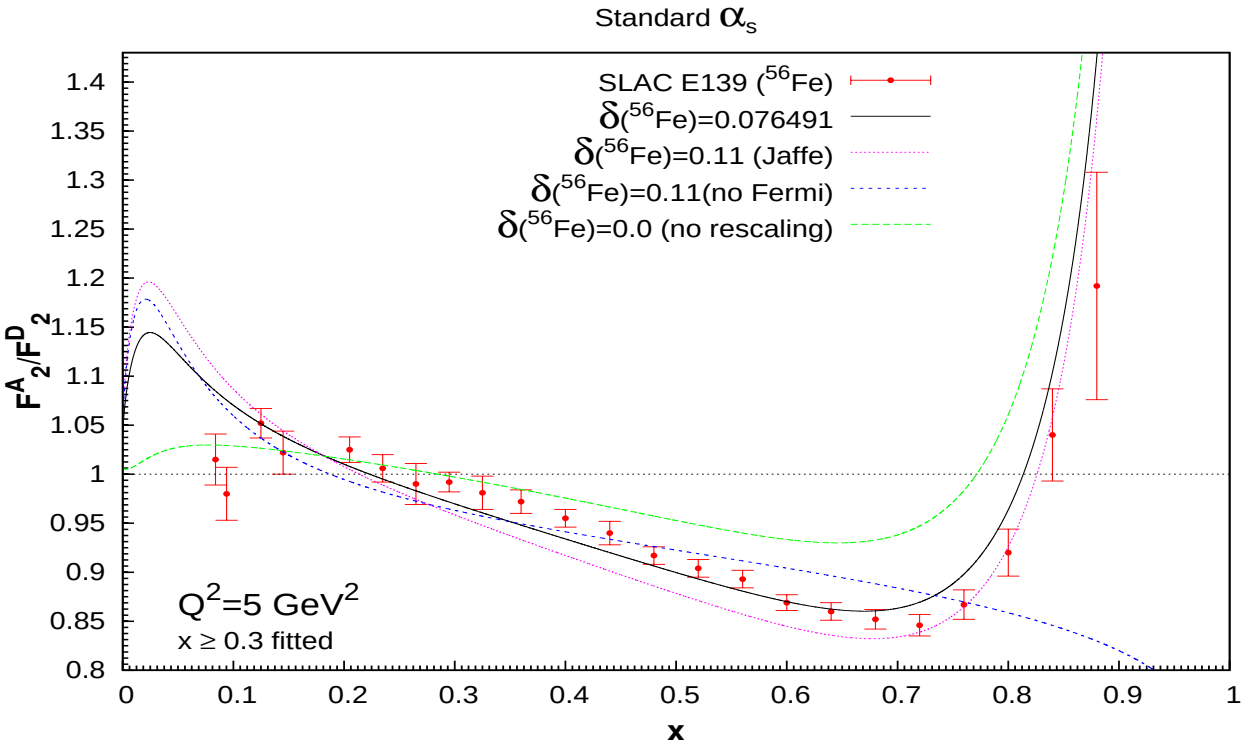

Figure 2: Same as in Fig.1 butg for the ratio $F_2^{Fe}(x,Q^2)/F_2^D(x,Q^2)$.

(S. Malace, D. Gaskell, D.W. Higinbotham, I. Cloet, 2014); (K. Rith, 2015)).

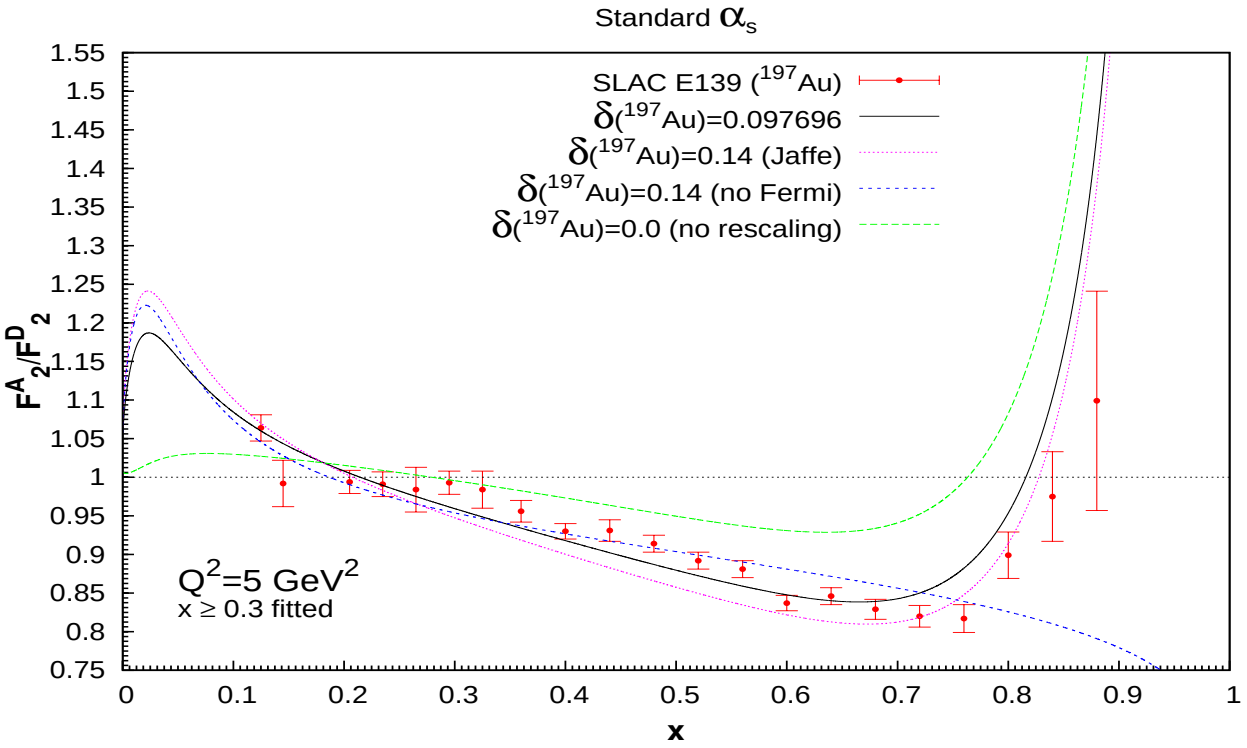

Figure 3: Same as in Fig.1 butg for the ratio $F_2^{Au}(x,Q^2)/F_2^D(x,Q^2)$.

It was first observed by the European Muon Collaboration (EMC) (J.J. Aubert et al.,1983)

in the valence quark dominance region $0.2 \leq x \leq 0.8$; hence the name.

This observation rules out the naive picture of a nucleus as being a system of quasi-free nucleons.

There in general are two mainstream approaches to studying the EMC effect.

- In the first one, which is at present more popular, nuclear parton distribution functions (nPDFs) are extracted from the global fits to nuclear data by using empirical parametrizations of their normalizations
  LO:(K.J. Eskola, H. Paukkunen, C.A.Salgado , 2009); (M. Hirai, S. Kumano, T.H. Nagai, 2007); (K. Kovarik $et\ al.$, nCTEQ15, 2015); NLO:(K.J. Eskola, P. Paukkunen, H. Paukkunen, C.A.Salgado, 2016); NNLO:(H. Khanpour and S. Atashbar Tehrani, 2016).
  This is completely analogous to respective studies of usual PDFs (L.A. Harland-Lang, A.D. Martin, P. Motylinski, R.S. Thorne,

2015); (R.D. Ball $et\ al.$, NNPDF Collab., 2015); (P. Jimenez-Delgado, E. Reya, 2014); (A. Accardi, L.T. Brady, W. Melnitchouk, J.F. Owens, N. Sato, 2016); (S. Alekhin, J. Blümlein, S. Moch, R. Placakyte, 2017).

Both PDFs and nPDFs are obtained from the numerical soution to Dokshitzer-Gribov-Lipatov-Altarelli-Parisi (DGLAP) equations (V.N. Gribov, L.N. Lipatov, 1972); (L.N. Lipatov, 1975); (G. Altarelli, G. Parisi, 1977); (Y.L. Dokshitzer, 1977).

- The second strategy is based upon some models of nuclear PDFs (see different models in, a recent review (S.A. Kulagin,2016)).

Here we will follow the $classical$ rescaling model
(R.L. Jaffe, F.E. Close, R.G. Roberts, G.G. Ross, 1983,1984, 1985);
(O. Nachtmann, H.J. Pirner, 1984),
which is based upon the suggestion
(R.L. Jaffe, F.E. Close, R.G. Roberts, G.G. Ross, 1983)
that the effective confinement size of gluons and quarks in the nucleus is greater than in a free nucleon.
In the framework of perturbative QCD it was found
(R.L. Jaffe, F.E. Close, R.G. Roberts, G.G. Ross, 1983,1984, 1985)
that such a change in the confinement scale predicts that nPDFs and PDFs can be related by simply rescaling their arguments.
Thus, in a sense, the rescaling model lies in-between two above approaches: in its framework there are certain relations between usual and nuclear PDFs that result from shifting the values of kinematical variable μ^2; however, both densities obey DGLAP equations.

At that time, the model was established for the valence quark dominance region: $0.2 \leq x \leq 0.8$.

The aim of our study is to extend its applicability to the region of small x values, where the rescaling values can be different for gluons and quarks.

We use the generalized double-scaling approach (DAS)
(L. Mankiewicz, A. Saalfeld, T. Weigl, 1997);
(A.V. Kotikov, G. Parente, 1999),
which is based upon the analytical solution to DGLAP equations in the small x region and generalizes earlier studies
(A. De Rújula, S.L. Glashow, H.D. Politzer, S.B. Treiman, F. Wilczek, A. Zee, 1974); (R.D. Ball, S. Forte, 1994).

Our present analysis
(A.V. Kotikov, B.G. Shaikhatdenov, Pengming Zhang, 2017)
is carried out to the LO accuracy.

We would like to note that such a low accuracy is used only for the present study, which can be considered as a first step in our investigations. We are going to improve the accuracy at least to the NLO level in the future works.

3 SF F_2 at low x

A reasonable agreement between HERA data and predictions made by perturbative QCD (pQCD) was observed for $Q^2 \geq 2$ GeV^2

(A.M. Cooper-Sarkar, R.C.E. Devenish, A. De Roeck, 1998);

(A.V. Kotikov, 2007),

thus promising that pQCD is capable of describing the evolution of parton densities down to very low Q^2 values.

Some time ago ZEUS and H1 Collaborations have presented new precise combined data
(F. D. Aaron $et\ al.$, H1 and ZEUS Collab.,2010)
on the structure function (SF) F_2.

An application of the generalized DAS approach at NLO
(A.V. Kotikov, G. Parente, 1999).
shows that theoretical predictions are well compatible with experimental data at $Q^2 \geq 3 \div 4$ GeV^2 (see recent results in
(A.V. Kotikov, and B.G. Shaikhatdenov, 2013, 2015, 2016))

We perform the LO analyses of the combined H1 and ZEUS data (A.V. Kotikov, B.G. Shaikhatdenov, Pengming Zhang, 2017), where the SF F_2 has the following form

$$F_2(x,\mu^2) = e\, f_q(x,\mu^2), \quad e = \sum_1^f \frac{e_i^2}{f}$$

where e is an average of the squared quark charges.

The small-x asymptotic expressions for parton densities f_a:

$$f_a(x,\mu^2) = f_a^+(x,\mu^2) + f_a^-(x,\mu^2), \quad (\text{hereafter} \quad a = q,g)$$

$$f_g^+(x,\mu^2) = (A_g + \frac{4}{9}A_q)\tilde{I}_0(\sigma)\, e^{-\overline{d}_+ s} + O(\rho),$$

$$f_q^+(x,\mu^2) = \frac{f}{9}(A_g + \frac{4}{9}A_q)\rho\tilde{I}_1(\sigma)\, e^{-\overline{d}_+ s} + O(\rho),$$

$$f_g^-(x,\mu^2) = -\frac{4}{9}A_q e^{-d_- s} + O(x), \quad f_q^-(x,\mu^2) = A_q e^{-d_-(1)s} + O(x),$$

where I_ν $(\nu = 0, 1)$ are the modified Bessel functions with

$$s = \ln\left(\frac{a_s(\mu_0^2)}{a_s(\mu^2)}\right), \quad \sigma = 2\sqrt{\left|\hat{d}_+\right| s \ln\left(\frac{1}{x}\right)}, \quad \rho = \frac{\sigma}{2\ln(1/x)},$$

$$a_s(\mu^2) \equiv \frac{\alpha_s(\mu^2)}{4\pi} = \frac{1}{\beta_0 \ln(\mu^2/\Lambda^2_{\rm LO})} \tag{2}$$

and

$$\hat{d}_+ = -\frac{12}{\beta_0}, \quad \overline{d}_+ = 1 + \frac{20f}{27\beta_0}, \quad d_- = \frac{16f}{27\beta_0} \tag{3}$$

denote singular $\hat{d}_+$ and regular $\overline{d}_+$ parts of the "anomalous dimensions" $d_+(n)$ and $d_-(n)$ respectively, in the limit $n \to 1$.

By using the above results we have analyzed H1 and ZEUS data for F_2. In order to keep the analysis as simple as possible, here we take $\mu^2 = Q^2$ and $\alpha_s(M_Z^2) = 0.1168$ in agreement with ZEUS results. Moreover, we use the fixed flavor scheme with two different values $f = 3$ and $f = 4$ of active quarks.

Table 1.

$f=3$	$a_s(Q^2)$	$a_s(Q^2)$	$a_{an}(Q^2)$	$a_{an}(Q^2)$	$a_{fr}(Q^2)$	$a_{fr}(Q^2)$
$Q^2 \geq$	1 GeV^2	3.5 GeV^2	1 GeV^2	3.5 GeV^2	1 GeV^2	3.5 GeV^2
A_g	0.46 ± 0.02	0.74 ± 0.04	1.16 ± 0.03	1.30 ± 0.04	0.96 ± 0.03	1.06 ± 0.04
A_q	1.58 ± 0.04	1.48 ± 0.06	1.16 ± 0.04	1.21 ± 0.07	1.23 ± 0.08	1.32 ± 0.07
Q_0^2	0.40 ± 0.01	0.46 ± 0.01	0.20 ± 0.01	0.16 ± 0.01	0.49 ± 0.01	0.53 ± 0.01
χ^2/N_{points}	365.7/67	69.7/37	149.7/67	42.9/37	140.4/67	47.6/37
$f=4$	$a_s(Q^2)$	$a_s(Q^2)$	$a_{an}(Q^2)$	$a_{an}(Q^2)$	$a_{fr}(Q^2)$	$a_{fr}(Q^2)$
$Q^2 \geq$	1 GeV^2	3.5 GeV^2	1 GeV^2	3.5 GeV^2	1 GeV^2	3.5 GeV^2
A_g	0.47 ± 0.02	0.54 ± 0.03	0.65 ± 0.02	0.76 ± 0.03	0.96 ± 0.03	0.77 ± 0.03
A_q	1.58 ± 0.04	1.09 ± 0.06	0.95 ± 0.03	0.96 ± 0.04	1.23 ± 0.05	0.95 ± 0.06
Q_0^2	0.40 ± 0.01	0.37 ± 0.01	0.16 ± 0.01	0.19 ± 0.01	0.49 ± 0.01	0.43 ± 0.01
χ^2/N_{points}	366.0/67	57.0/37	166.3/67	43.6/37	140.0/67	40.6/37

As can be seen from Table 1, the twist-two approximation looks reasonable for $Q^2 \geq 3.5$ GeV^2. It is almost completely compatible with NLO analyses

(A.V. Kotikov, and B.G. Shaikhatdenov, 2013, 2015, 2016).

Moreover, these results are rather close to original analyses (A.M. Cooper-Sarkar *et al.*, 2016); (I. Abt *et al.*, 2016), performed by the HERAPDF group.

At lower Q^2 there is certain disagreement, which is we believe to be explained by the higher-twist (HT) corrections playing their important role.

These HT corrections have rather cumbersome form at low x (A.Yu. Illarionov, A.V. Kotikov, G. Parente, 2007).

It is very promising to use infrared modifications of the strong coupling constant in our analysis.

(Cvetic, A.Yu. Illarionov, B.A. Kniehl, A.V. Kotikov, 2009),

Such types of coupling constants modify the low μ^2 behavior of parton densities and structure functions. What is important, they do not produce additional free parameters.

We use "frozen" $a_{\rm fr}(\mu^2)$

(B. Badelek, J. Kwiecinski, A. Stasto, 1997), (Y.A. Simonov, 2011)

and analytic $a_{\rm an}(\mu^2)$ (D.V. Shirkov, I.L. Solovtsov, 1997)

versions

$$a_{\rm fr}(\mu^2) = a_s(\mu^2 + M_g^2), \quad a_{\rm an}(\mu^2) = a_s(\mu^2) - \frac{1}{\beta_0}\frac{\Lambda^2_{\rm LO}}{\mu^2 - \Lambda^2_{\rm LO}}, \quad (4)$$

where M_g is a gluon mass with M_g=1 GeV^2.

It is seen that the results of the fits carried out when $a_{\rm fr}(\mu^2)$ and $a_{\rm an}(\mu^2)$ are used, are very similar to the corresponding NLO ones. Moreover, note that the fits in the cases with "frozen" and analytic strong coupling constants look very much alike and describe fairly well the data in the low Q^2 region, as opposed to the fits with a standard coupling constant, which largely fails here. The results are presented in Table 1. With the number of active quarks $f = 4$, they are shown also in Fig. 1.

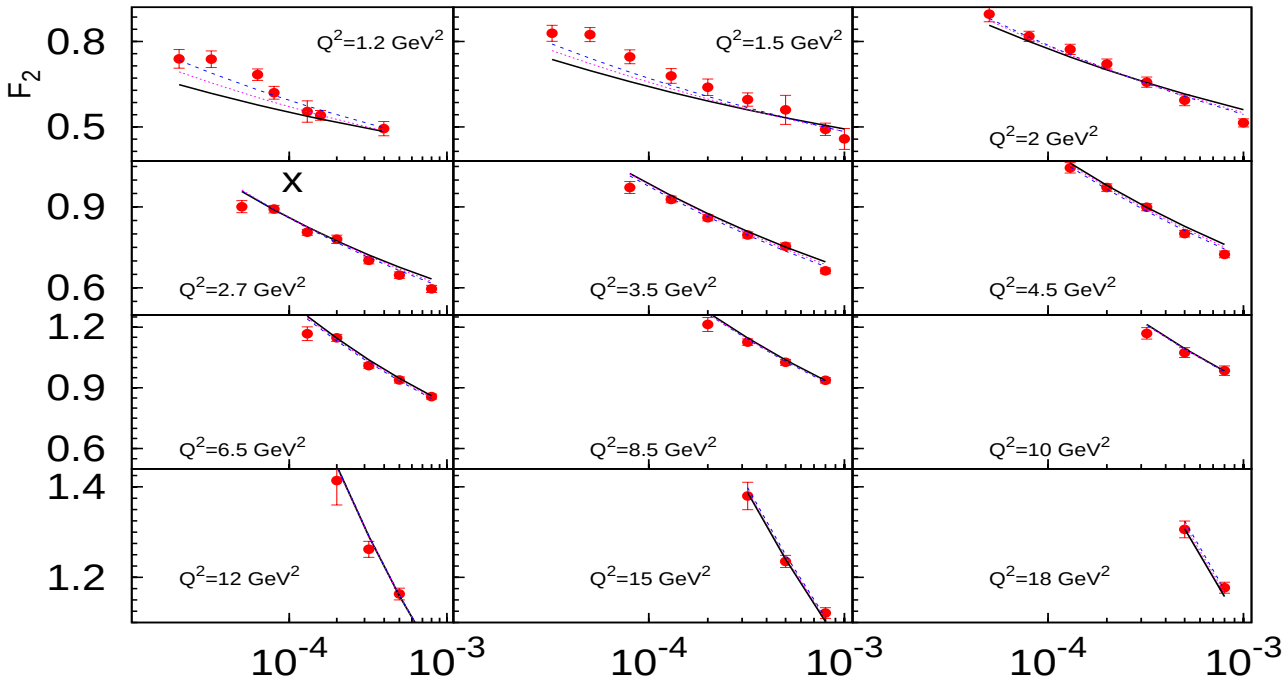

Figure 4: x dependence of $F_2(x, Q^2)$ in bins of Q^2. The combined experimental data from H1 and ZEUS Collaborations are compared with the LO fits for $Q^2 \geq 1$ GeV^2 implemented with the standard (solid lines), frozen (dash-dotted lines), and analytic (dashed lines) modifications of the strong coupling constant.

Just like the previous NLO analyses we observe strong improvement in the agreement between theoretical predictions and experimental data once "frozen" and analytic modifiations to the coupling constant are applied: χ^2 value drops by more than two times.

4 Rescaling model

In the rescaling model SF F_2 and, therefore, valence part of quark densities, gets modified in the case of a nucleus A at intermediate and large x values $(0.2 \leq x \leq 0.9)$ as follows

$$F_2^A(x,\mu^2) = F_2(x,\mu^2_{A,v}), \quad f^A_{NS}(x,\mu^2) = f_{NS}(x,\mu^2_{A,v}),$$

where a new scale $\mu^2_{A,v}$ is related with μ^2 as

$$\mu^2_{A,v} = \xi_v^A(\mu^2)\mu^2, \quad \xi_v^A(\mu^2) = \left(\frac{\lambda_A^2}{\lambda_N^2}\right)^{a_s(\tilde{\mu}^2)/a_s(\mu^2)},$$

where some additional scale $\tilde{\mu}^2 = 0.66$ GeV^2, which in-turn was the initial condition for an μ^2-evolution.

The values of λ_A/λ_N and $\xi_v^A(\mu^2)$ at $\mu^2 = 20$ GeV^2 were evaluated for different nuclei and presented in Tables I and II in (F.E. Close, R.L. Jaffe, R.G. Roberts, G.G. Ross, 1985).

Since the factor $\xi_v^A(\mu^2)$ is μ^2 dependent, it is convenient to transform it to some μ^2 independent one.

We consider the variable $\ln(\mu^2_{A,v}/\Lambda^2)$

$$\ln\left(\frac{\mu^2_{A,v}}{\Lambda^2}\right) = \ln\left(\frac{\mu^2}{\Lambda^2}\right) \cdot (1 + \delta_v^A)$$

where the nuclear correction factor δ_v^A becomes μ^2 independent:

$$\delta_v^A = \frac{1}{\ln\left(\tilde{\mu}^2/\Lambda^2\right)} \ln\left(\frac{\lambda_A^2}{\lambda_N^2}\right),$$

where we see that two parameters: the scale $\tilde{\mu}$ and the ratio λ_A/λ_N, form the the Q^2-independent combination.

The results for δ_v^A are presented in Table 2.

Table 2.

A	^{2}D	^{4}He	^{7}Li	^{12}C	^{40}Ca
N		11	16	16	11
δ_v^A	0.01	0.06	0.05	0.08	0.11
δ_v^{AD}	0	0.05	0.04	0.07	0.10
$-\delta_{+,an}^{AD}$	0	0.06 ± 0.01	0.06 ± 0.01	0.11 ± 0.01	0.19 ± 0.01
$-\delta_{-,an}^{AD}$	0	0.24 ± 0.08	0.22 ± 0.07	0.41 ± 0.04	0.51 ± 0.04
χ_{an}^2	0	4.68	17	9.68	12
$-\delta_{+,fr}^{AD}$	0	0.06 ± 0.01	0.06 ± 0.01	0.12 ± 0.01	0.21 ± 0.02
$-\delta_{-,fr}^{AD}$	0	0.32 ± 0.08	0.28 ± 0.07	0.54 ± 0.04	0.71 ± 0.04
χ_{fr}^2	0	5	35	26	37

Since our parton densities contain the variable s. it is convenient to consider its A modification:

$$s_v^A \equiv \ln\left(\frac{\ln\left(\mu_{A,v}^2/\Lambda^2\right)}{\ln\left(\mu_0^2/\Lambda^2\right)}\right) = s + \ln(1+\delta_v^A) \approx s + \delta_v^A,$$

i.e. the nuclear modification of the basic variable s depends on the μ^2 independent parameter δ_v^A, which possesses very small values.

5 Rescaling model al low x

Standard evidence coming from earlier studies contains conclusion about inapplicability of the rescaling model at small x values (see, for example, (A.V. Efremov, 1986))

It looks like it can be related with some simplifications of low x analyses, where the rise in EMC ratio was wrongly predicted at small x values.

(see, for example, (A.V. Kotikov, 1988))

Using an accurate study of DGLAP equations at low x within the framework of the generalized DAS approach, it is possible to achieve nice agreement with the experimental data for the DIS structure functon F_2 (see above). Therefore, we believe that all these indicate toward success in study of **the DIS structure functon** F_2^A and, thus, the EMC ratio by using the same approach.

Thus, we are trying to apply the DAS approach to low x region of EMC effect using a simple fact that the rise of parton densities increases with increasing Q^2 values. This way, with scales of PDF evolutions less than Q^2 (i.e. $\mu_A^2 \leq Q^2$ for gluons and sea quarks) in nuclear cases, we can directly reproduce the shadowing effect which is observed in the global fits. Since there are two components for each parton density, we have two free parameters $\mu_\pm$ to be fit in the analyses of experimental data for EMC effect at low x values.

Application of the rescaling model at low x at LO:

$$
\begin{aligned}
F_2^A(x,\mu^2) &= e\, f_q^A(x,\mu^2), \quad F_2^N(x,\mu^2) = e\, f_q(x,\mu^2), \\
f_a^A(x,\mu^2) &= f_a^{A,+}(x,\mu^2) + f_a^{A,-}(x,\mu^2), \quad (a = q, g), \\
f_a^{A,\pm}(x,\mu^2) &= f_a^{\pm}(x,\mu^2_{A,\pm})\,,
\end{aligned}
$$

with a similar definition of $\mu^2_{A,\pm}$ as above for $\mu^2_{A,v}$ (up to replacement $v \to \pm$).

Then, the corresponding values of $s^A_\pm$ are found to be

$$
s^A_\pm \equiv \ln\left(\frac{\ln\left(\mu^2_{A,\pm}/\Lambda^2\right)}{\ln\left(\mu^2_0/\Lambda^2\right)}\right) = s + \ln(1+\delta^A_\pm)\,,
$$

because of the saturation at low x values for all considered Q^2 values, which in our case should be related with decreasing the arguments of "$\pm$" component. Therefore, the values of $\delta^A_\pm$ should be negative.

6 Analysis of the low x data for nucleus

Note that it is usually convenient to study the following ratio

$$R_{F2}^{AD}(x,\mu^2) = \frac{F_2^A(x,\mu^2)}{F_2^D(x,\mu^2)}\,.$$

Using the fact that the nuclear effect in a deutron is very small (see Table 1 for the values of δ_v^A) , we can suggest that

$$\begin{aligned}
F_2^D(x,\mu^2) &= e\, f_q(x,\mu^2), \quad F_2^A(x,\mu^2) = e\, \overline{f}_q^A(x,\mu^2), \\
\overline{f}_a^A(x,\mu^2) &= \overline{f}_a^{A,+}(x,\mu^2) + \overline{f}_a^{A,-}(x,\mu^2), \quad (a = q, g), \\
\overline{f}_a^{A,\pm}(x,\mu^2) &= f_a^{\pm}(x,\mu^2_{AD,\pm})\,,
\end{aligned}$$

i.e.

$$
\begin{aligned}
\overline{f}_g^{A,+}(x,\mu^2) &= (A_g + \frac{4}{9}A_q) I_0(\sigma_+^{AD})\, e^{-\bar{d}_+ s_+^{AD}} + O(\rho_+^{AD}), \\
\overline{f}_q^{A,+}(x,\mu^2) &= \frac{f}{9}(A_g + \frac{4}{9}A_q)\rho_+^{AD} I_1(\sigma_+^{AD})\, e^{-\bar{d}_+ s_+^{AD}} + O(\rho_+^{AD}), \\
\overline{f}_g^{A,-}(x,\mu^2) &= -\frac{4}{9}A_q e^{-d_- s_-^{AD}} + O(x), \\
\overline{f}_q^{A,-}(x,\mu^2) &= A_q e^{-d_-(1) s_-^{AD}} + O(x),
\end{aligned}
$$

where

$$
\sigma_+^{AD} = \sigma(s \to s_+^{AD}), \quad \rho_+^{AD} = \rho(s \to s_+^{AD}),
$$

$$
s_\pm^{AD} \equiv \ln\left(\frac{\ln\left(\mu_{AD,\pm}^2/\Lambda^2\right)}{\ln\left(\mu_0^2/\Lambda^2\right)}\right) = s + \ln(1+\delta_\pm^{AD})\,.
$$

We obtain the values of $\delta_{\pm}^{AD}$ by fitting NMC experimenal data (M. Arneodo *et al.*, New Muon Collab.,1995) for the EMC ratio at low x in the case of different nuclei.

Since the experimental data for lithium and carbon are most precise and contain the maximal number of points (16 points for each nucleus), we preform combined fits of these data. Obtained results (with χ^2_{an}=27 and χ^2_{fr}=43 for 32 points) are presented in Table 3 and shown in Fig. 2.

Table 3.

	$-\delta^{AD}_{+,an}$	$-\delta^{AD}_{-,an}$	$-\delta^{AD}_{+,fr}$	$-\delta^{AD}_{-,fr}$
^{7}Li	0.061 ± 0.006	0.216 ± 0.065	0.073 ± 0.012	0.348 ± 0.067
^{12}C	0.105 ± 0.007	0.411 ± 0.042	0.139 ± 0.013	0.590 ± 0.041

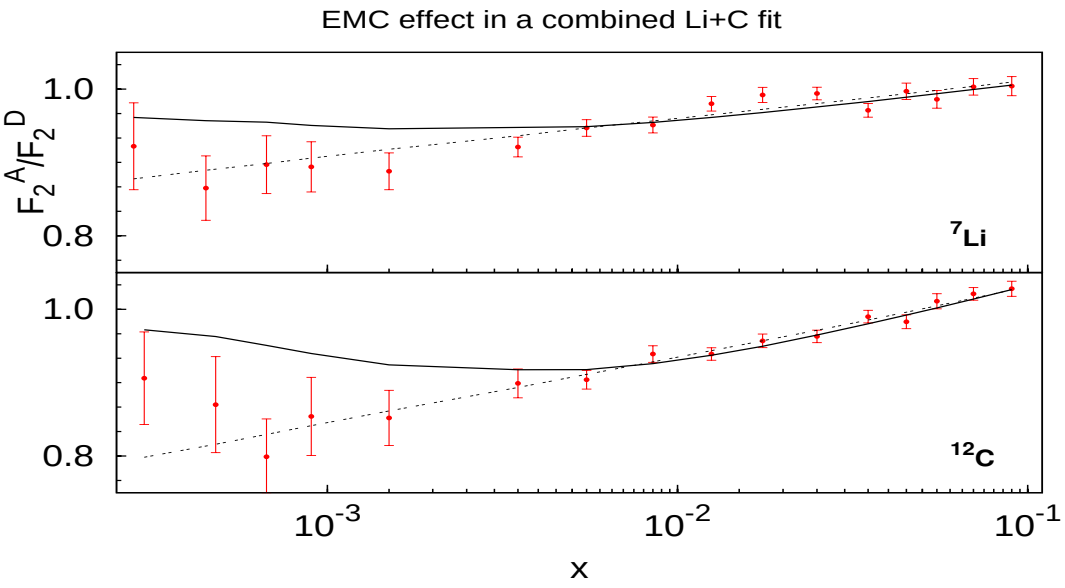

Figure 5: x dependence of $R_a^{AD}(x,\mu^2)$ in bins of x. The combined experimental data from NMC are compared with the LO fits implemented with the frozen (solid lines) and analytic (dashed lines) modifications of the strong coupling constant.

As can be seen in Fig. 2 there is large difference between the fits with "frozen" and analytic versions of the strong couling constant. This is in contrast with the analysis done above for SF F_2.

This difference comes about because we include in the analysis the region of very low Q^2 values, where "frozen" and analytic strong couling constants are rather different (D.V. Shirkov, 2012)).

6 A dependence at low x

Taking NMC experimental data

(M. Arneodo *et al.*„ 1995), (P. Amaudruz *et al.*, 1995)

along with E665 and HERMES Collaborations

(M.R. Adams *et al.*, E665 Collab., 1995);

(K. Ackerstaff *et al.*, HERMES Collab., 2000)

for the EMC ratio at low x in the case of different nuclei, we can find the A dependence of $\delta_{\pm}^{AD}$, in the form

$$-\delta_{\pm}^{AD} = c_{\pm}^{(1)} + c_{\pm}^{(2)} A^{1/3}.$$

The values of $c_{\pm}^{(1)}$ and $c_{\pm}^{(2)}$ are found in the combined fit of the data (76 points) with the analytic coupling constant (with $\chi^2 = 89$)

$$c_{+,an}^{(1)} = -0.055 \pm 0.015, \quad c_{+,an}^{(2)} = 0.068 \pm 0.006,$$
$$c_{-,an}^{(1)} = 0.071 \pm 0.101, \quad c_{-,an}^{(2)} = 0.120 \pm 0.039\,.$$

Now, using the above A dependence, $R_{F2}^{AD}(x,\mu^2)$ values for any nucleus A can be predicted.

What is more, we can consider also the ratios $R_a^{AD}(x,\mu^2)$ of parton densities in a nucleus and deutron themselves,

$$R_a^{AD}(x,\mu^2) = \frac{\overline{f}_a^A(x,\mu^2)}{f_a(x,\mu^2)}, \quad (a = q, g)\,,$$

Indeed, at LO $R_q^{AD}(x,\mu^2) = R_{F2}^{AD}(x,\mu^2)$; therefore, results for $R_q^{AD}(x,\mu^2)$ are already known. Since all the parameters of PDFs found within the framework of the generalized DAS approach are now fixed we can predict the ratio $R_g^{AD}(x,\mu^2)$ of the gluon densities in a nucleus and nucleon, which is currently under intensive studies (see a recent review

(N. Armesto, 2006)

along with references and discussion therein).

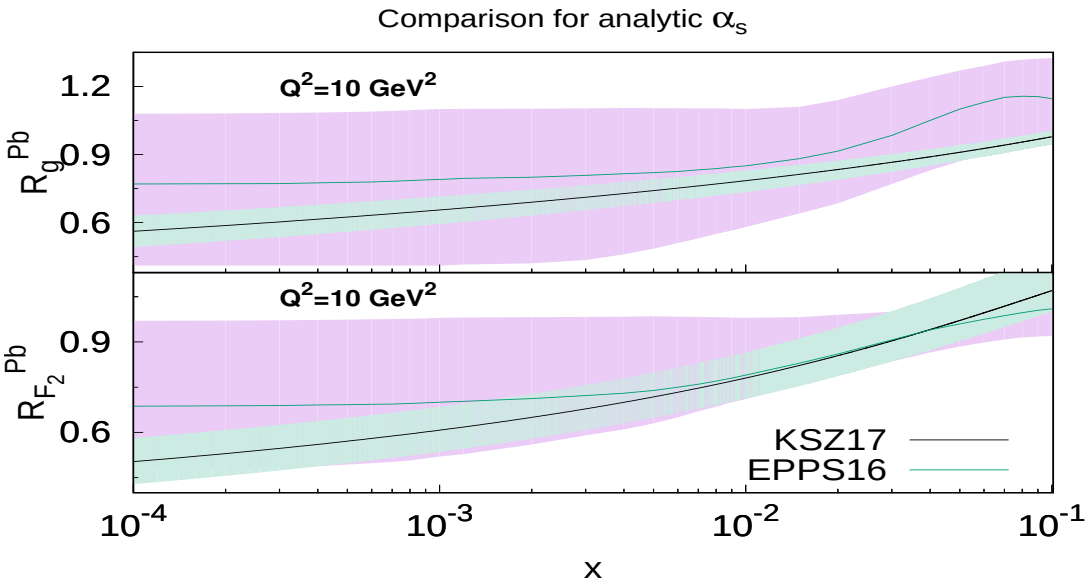

Figure 6: x dependence of $R_{F2}^{AD}(x,\mu^2)$ and $R_g^{AD}(x,\mu^2)$ at μ^2=10 GeV^2 in x bins for lead data. Pink and blue bands show 90% uncertainties taken from (H. Paukkunen, 2017) respectively. The red line shows their result and the black one is obtained in the present paper.

The results for $R_{F2}^{AD}(x,\mu^2)$ and $R_g^{AD}(x,\mu^2)$, depicted in Fig. 3, show some difference between these ratios. The difference is similar to that obtained in the recent EPPS16 analysis (K.J. Eskola, P. Paakkinen, H. Paukkunen, C.A. Salgado, 2017).

However, what for $R_{F2}^{AD}(x,\mu^2)$ and $R_g^{AD}(x,\mu^2)$ themselves, we obtain a bit stronger effect at lowest x values, which does in fact not contradict the experimental data collected by the LHCb experiment (see recent review in (M. Winn, 2017).

Such a strong effect is also well compatible with the leading order EPPS09 analysis (which can also be found in above paper).

As the end, we would to put some note about the uncertantity bands. The results for $R_g^{AD}(x, \mu^2)$ together with the blue band is completely determined by the rescaling model and our analytic form of parton densities at low x values. So, the blue band for $R_g^{AD}(x, \mu^2)$ should strongly increae in the case of a freedom in an usage of various models. Moreover, a comparizon between two above bands is ruther misleading. The pink band is much broader since the EPPS16 global analysis included a fit to all available data but not just some small x ones as it was done here.

7 Conclusion

We applied the DAS approach to examine an EMC F_2 structure function ratio between various nuclei and a deutron.

- Within a framework of the rescaling model good agreement between theoretical predictions and experimental data is achieved.
- The theoretical formullas contain certain parameters, whose values were fitted in the analyses of experimental data. Once the fits are carried out we have predictions for the corresponding ratios of parton densities without free parameters. These results were used to predict small x behavior of the gluon density in nuclei, which is at present poorly known.
- The obtained ratios $R_a^{AD}(x,\mu^2)$ $(a = q, g)$ are compatible with those given by various groups working in the area. The rescaling model provided us with very simple forms for these ratios.

FUTURE

- We plan to extend our analysis to the NLO level of approximation, the accuracy that is currently a standard in nPDF studies.
- Using the parametrizations of parton valence density in (A.Y. Illarionov, A.V. Kotikov, S.S. Parzycki, D.V. Peshekhonov, 2011), we plan to apply the rescaling model to study the structure function xF_3.
- We are going to consider a rather broad range of the Bjorken variable x by using parametrizations of parton densities, which will be constructed by analogy with the above one.
  The usage of such type of parametrizations give a possibility to study the range of intermediate x values, which is presently under active considerations.